Earth and Planetary Science Letters 366 (2013) 49–58

Contents lists available at SciVerse ScienceDirect

Earth and Planetary Science Letters

journal homepage: www.elsevier.com/locate/epsl

Lowland river responses to intraplate tectonism and climate forcing quantified with luminescence and cosmogenic ^{10}Be

J.D. Jansen [a,*], G.C. Nanson [b], T.J. Cohen [b], T. Fujioka [c], D. Fabel [d], J.R. Larsen [e], A.T. Codilean [b], D.M. Price [b], H.H. Bowman [b], J.-H. May [b], L.A. Gliganic [b]

[a] Department of Physical Geography and Quaternary Geology, Stockholm University, 106 91 Stockholm, Sweden
[b] School of Earth and Environmental Sciences, University of Wollongong, Wollongong 2500, Australia
[c] Institute for Environmental Research, Australian Nuclear Science and Technology Organisation, Lucas Heights 2234, Australia
[d] School of Geographical and Earth Sciences, University of Glasgow, Glasgow G12 8QQ, UK
[e] School of Geography, Planning, and Environmental Management, University of Queensland, St Lucia 4072, Australia

ARTICLE INFO

Article history:
Received 21 January 2013
Received in revised form
11 February 2013
Accepted 11 February 2013
Editor: T.M. Harrison
Available online 19 March 2013

Keywords:
intraplate tectonism
bedrock river incision
anabranching
cosmogenic nuclides
luminescence
deposition rate

ABSTRACT

Intraplate tectonism has produced large-scale folding that steers regional drainage systems, such as the 1600 km-long Cooper Ck, en route to Australia's continental depocentre at Lake Eyre. We apply cosmogenic ^{10}Be exposure dating in bedrock, and luminescence dating in sediment, to quantify the erosional and depositional response of Cooper Ck where it incises the rising Innamincka Dome. The detachment of bedrock joint-blocks during extreme floods governs the minimum rate of incision (17.4 ± 6.5 mm/ky) estimated using a numerical model of episodic erosion calibrated with our ^{10}Be measurements. The last big-flood phase occurred no earlier than ~112–121 ka. Upstream of the Innamincka Dome long-term rates of alluvial deposition, partly reflecting synclinal-basin subsidence, are estimated from 47 luminescence dates in sediments accumulated since ~270 ka. Sequestration of sediment in subsiding basins such as these may account for the lack of Quaternary accumulation in Lake Eyre, and moreover suggests that notions of a single primary depocentre at base-level may poorly represent lowland, arid-zone rivers. Over the period ~75–55 ka Cooper Ck changed from a bedload-dominant, laterally-active meandering river to a muddy anabranching channel network up to 60 km wide. We propose that this shift in river pattern was a product of base-level rise linked with the slowly deforming syncline–anticline structure, coupled with a climate-forced reduction in discharge. The uniform valley slope along this subsiding alluvial and rising bedrock system represents an adjustment between the relative rates of deformation and the ability of greatly enhanced flows at times during the Quaternary to incise the rising anticline. Hence, tectonic and climate controls are balanced in the long term.

1. Introduction

River response to tectonic deformation determines local relief and the supply of sediment to basins. Surface uplift may steepen rivers, increasing their erosional capacity to incise bedrock and transport sediment, but the converse also occurs, for instance, where rising transverse structures cause deposition and possible river diversion (Schumm et al., 2000). In the case of low relief landscapes, the sensitivity to small changes in slope means that anomalous river patterns may be the first clue to tectonic activity (e.g. Nanson, 1980). Intraplate tectonism has notably perturbed sections of large lowland rivers such as the Amazon and Mississippi chiefly because such rivers flow across very low gradients (Adams, 1980; Holbrook and Schumm, 1999). Whether a river is diverted or maintains course by incising in pace with uplift is held to be a function of the surface uplift rate, sediment flux, and stream power relative to critical thresholds of erosion (Schumm et al., 2000), though the role of the latter has been questioned (Humphrey and Konrad, 2000). Stream power fluctuations in large, low-gradient rivers are primarily a function of flood magnitude, yet episodic bedrock erosion via extreme floods has barely been examined in large lowland rivers. Much of what is known of how such rivers respond to transverse uplift derives from simplified scenarios explored via physical and numerical modelling (e.g., Humphrey and Konrad, 2000; Molnar et al., 2006), with flume experiments, in particular, contributing major insights to the effects of transverse uplift, such as changes in sinuosity and planform style (Ouchi, 1985; Schumm et al., 1987). Although such observations have been corroborated qualitatively in natural

* Correspondence to: School of Earth and Environmental Sciences, University of Wollongong, Wollongong 2500, Australia.
Tel.: +61 2 4263 1274; fax: +61 2 4221 4250.
E-mail addresses: jjansen@uow.edu.au, john.jansen@natgeo.su.se (J.D. Jansen).

0012-821X/$ - see front matter © 2013 Elsevier B.V. All rights reserved.
http://dx.doi.org/10.1016/j.epsl.2013.02.007

rivers (e.g. Nanson, 1980; Holbrook and Schumm, 1999), there is rarely sufficient constraint on the magnitude of deformation and the associated river responses to fully evaluate a natural experiment over 10^5–10^6 y timescales.

A transverse structure rising across the path of an unconfined river is generally predicted to cause deposition upstream of the uplift axis at the same time as erosion downstream (Ouchi, 1985; Humphrey and Konrad, 2000). To test this idea, we examine both modes of fluvial response along a large, lowland river in east-central Australia, Cooper Ck, where it crosses the anticline known as Innamincka Dome (Fig. 1). The rate of alluvial deposition is quantified with luminescence dating, and bedrock incision with in situ cosmogenic ^{10}Be. Based on analyses of (i) river profile and planform, (ii) spatial patterns of short and long-term deposition rates, and (iii) rates of bedrock channel incision, we show that climate-driven flooding episodes over the last glacial cycle play a key role in how rivers adjust to intraplate tectonism, whilst sediment load appears secondary.

2. Field setting: tectonism and drainage evolution of east-central Australia

The subdued relief across east-central Australia implies a relatively quiescent tectonic regime accordant with reports of low denudation rates <10 mm/ky based on cosmogenic nuclide measurements of bedrock surfaces in central Australia (e.g., Bierman and Caffee, 2002; Belton et al., 2004; Heimsath et al., 2010; Fujioka and Chappell, 2011). Yet, the continent as a whole has experienced appreciable Neogene–Quaternary tectonism given its intraplate setting (Sandiford et al, 2009). Surface uplift has generated major local relief in the Flinders Ranges where reverse faulting drives Plio-Quaternary slip rates of 20–150 mm/ky (Sandiford, 2003). The gross regional drainage patterns of east-central Australia are rooted in this Neogene–Quaternary tectonism, involving an array of low-amplitude, open fold structures (Senior et al., 1978; Wasson, 1983; Wells and Callen, 1986; Alley, 1998). Intraplate tectonism in Australia is attributed to far-field stresses at the plate-boundary coupled with upper mantle dynamics (Sandiford et al., 2004). The regional in situ stress field in east-central Australia has a maximum horizontal compressive stress azimuth running NE to SW (Hillis et al., 2008), a pattern that probably dates from at least the mid to late Miocene (Sandiford et al., 2004), explaining the orientation of synclinal structures that steer Cooper Ck and associated drainages for ~700 km. In its middle and lower reaches, Cooper Ck dissects two anticlinal structures formed in Mesozoic Eromanga Basin rocks: Innamincka Dome and Gason–Cooryanna Domes, which together exert major influence on landscape evolution east of the intra-continental depocentre at Lake Eyre (Fig. 1A). The wavelength of folding is ~20–50 km, and Tertiary uplift is estimated at ~200 m (Wopfner et al., 1974; Moussavi-Harami and Alexander, 1998), with neotectonism inferred by the thinning of Pliocene–Quaternary sediments over buried structures west of Innamincka Dome (Wasson, 1983; Moussavi-Harami and Alexander, 1998). Rates of Quaternary deformation however are not known, though impacts on river systems have been inferred (Rust, 1981; Rust and Nanson, 1986; Nanson et al., 2008; Waclawik et al., 2008).

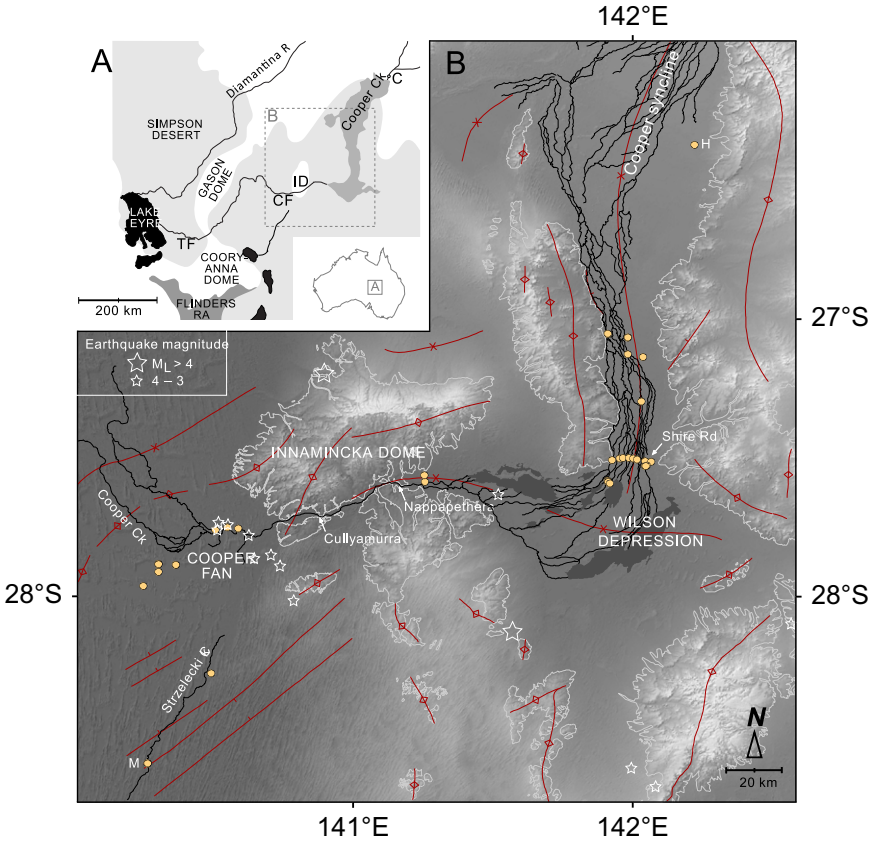

Fig. 1. (A) Field area in east-central Australia (modified after Wells and Callen (1986)), with Innamincka Dome (ID), Cooper Fan (CF), Tirari Fan (TF), Currareva (C), plus Cooper floodplain (mid-grey), and major playas (black). (B) 450 km-long reach of Cooper Ck centred on Innamincka Dome. Yellow filled-circles denote sites of measured deposition rates from Mt Howitt (H) to Merty Merty (M); dark-grey fills denote seasonal swamps. Stars denote earthquake epicentres $M_L > 3$ (Geoscience Australia earthquake database, 1961–2012). Grey outlines show extent of Cretaceous (Winton Fm) and Tertiary rocks (Eyre/Glendower Fm), red lines denote anticlines/synclines (triangles indicate dip-direction) and major faults (stem indicates down-throw) (Senior, 1969, 1970; Galloway et al., 1971; Townsend and Thornton, 1975; Gravestock et al., 1995). (For interpretation of the references to colour in this figure legend, the reader is referred to the web version of this article.)

2.1. Cooper Creek and Innamincka Dome

Cooper Ck drains ~300,000 km^2 of dryland east-central Australia. From the western slopes of the Great Dividing Range the Cooper flows ~1600 km inland to Lake Eyre, a large terminal playa draining ~14% of the continent (Fig. 1A). Mean annual rainfall ranges from 400–500 mm in the headwaters to <100 mm at Lake Eyre. Flow is highly seasonal with long dry spells of low or zero flow interspersed by high-magnitude flooding linked to the Indo-Australian monsoon and the southeast trade-winds, both of which are modulated by the El Niño-Southern Oscillation (Kotwicki, 1986; Nanson et al., 2008). Considered to be the largest flood for >100 yr (Kotwicki, 1986), the February 1974 peak discharge was 24,970 m^3/s at Currareva, and 6360 m^3/s ~400 km downstream at Cullyamurra (Fig. 1A,B), signifying ~75% transmission losses during this single event (Knighton and Nanson, 2002).

Channel slope rarely exceeds 200 mm/km and longitudinal transitions in river style define three reach segments: (1) the Cooper–Wilson synclinal depression, a vast anabranching channel system 400 km long and up to 60 km wide; (2) Innamincka Dome, a mainly single-thread mixed bedrock-alluvial channel with sporadic bedrock constrictions; and (3) Cooper Fan, which directs drainage into several unconfined distributary channels with varying degrees of entrenchment (Fig. 1B). Valley width contracts approaching the Innamincka Dome, and bedrock is first met at Nappapethera waterhole where a single-thread Cooper Ck becomes confined between bedrock banks with thin alluvial cover (Fig. 1B).

The local bedrock comprises Eyre Formation (Palaeocene to Eocene) quartzose sandstones underlain by Winton Formation (Cretaceous) kaolinitic shales and sandstones (Wopfner et al., 1974)—all mildly folded with limbs dipping at 1–5°. A silicified palaeosol developed prior to folding has formed a highly resistant silcrete duricrust sharply reflected in valley constrictions culminating at the upstream end of Cullyamurra waterhole where flow converges to ~30 m width (Fig. 1B). Such bedrock constrictions serve to amplify the erosional capacity of large floods, and field observations confirm that large joint-blocks are episodically plucked from bedrock outcrops (Fig. 2). Numerous large blocks (up to 1.1 m *b*-axis) are perched on bedrock surfaces flanking Cullyamurra waterhole, many bearing unambiguous evidence of flipping (e.g., inverted pot holes). The presence of such high-energy deposits in this very low gradient and arid region motivates our efforts to determine the timing and magnitude of floods necessary to erode bedrock and maintain course across the rising anticline.

3. Methods

3.1. River profile and modern flood dynamics

The longitudinal stream profile (Fig. 3A, B) was devised for Cooper Ck based on the Shuttle Radar Topography Mission (SRTM, 1 arc-s) digital elevation data (Supplementary Data, S1). Valley cross-sections were measured at key bedrock constrictions in the field with a differential GPS (Trimble R7/R8), and Cullyamurra waterhole bathymetry was surveyed using a boat-mounted echo-sounder (Fig. 3C). The flow geometry detailed in 50 field-measured cross-sections was used to calibrate the HEC-RAS hydraulic model (HEC, 1997) through an 8 km reach, including the bedrock constriction at Cullyamurra waterhole (Supplementary Data, S2). The 1974 peak discharge at Cullyamurra (6360 m^3/s, ~32-times the median annual flood) was simulated with the aim of estimating the erosional capacity of present-day big floods. Komar's (1996) selective entrainment function, a modified form of the Shields function, was employed to estimate the critical shear stress (τ_c, N/m^2) necessary for boulder mobility (cf. Jansen, 2006):

$$\tau_c = 0.045(\rho_s - \rho) g d_{50}^{0.6} d^{0.4} \quad (1)$$

where ρ_s is boulder density (2650 kg/m^3), ρ fluid density (1000 kg/m^3), g gravity (9.8 m/s^2), d clast size (mm), and d_{50} the median size of surrounding clasts (assumed to be 500 mm).

3.2. Deposition rates quantified via OSL–TL dating and sediment load data

An inventory was compiled of 132 sedimentary units dated with optically-stimulated luminescence (OSL) and thermoluminescence (TL) from 80 natural exposures and drill-holes (Rust and

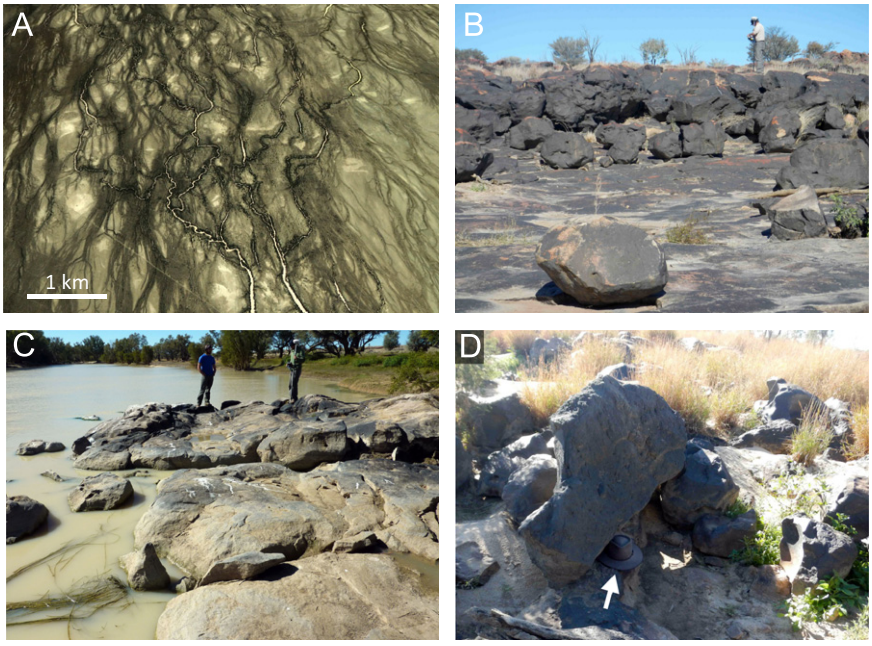

Fig. 2. (A) Oblique aerial Google Earth image of Cooper Ck anabranching channels upstream of Innamincka Dome, near Meringhina waterhole (flow top to bottom). (B) Stepped bedrock morphology at Choke transect (Cullyamurra waterhole); foreground boulder is ~1 m in diameter. (C) Abraded and plucked bedrock surface at Choke. (D) Imbricated boulder slab at Choke, with hat (arrowed).

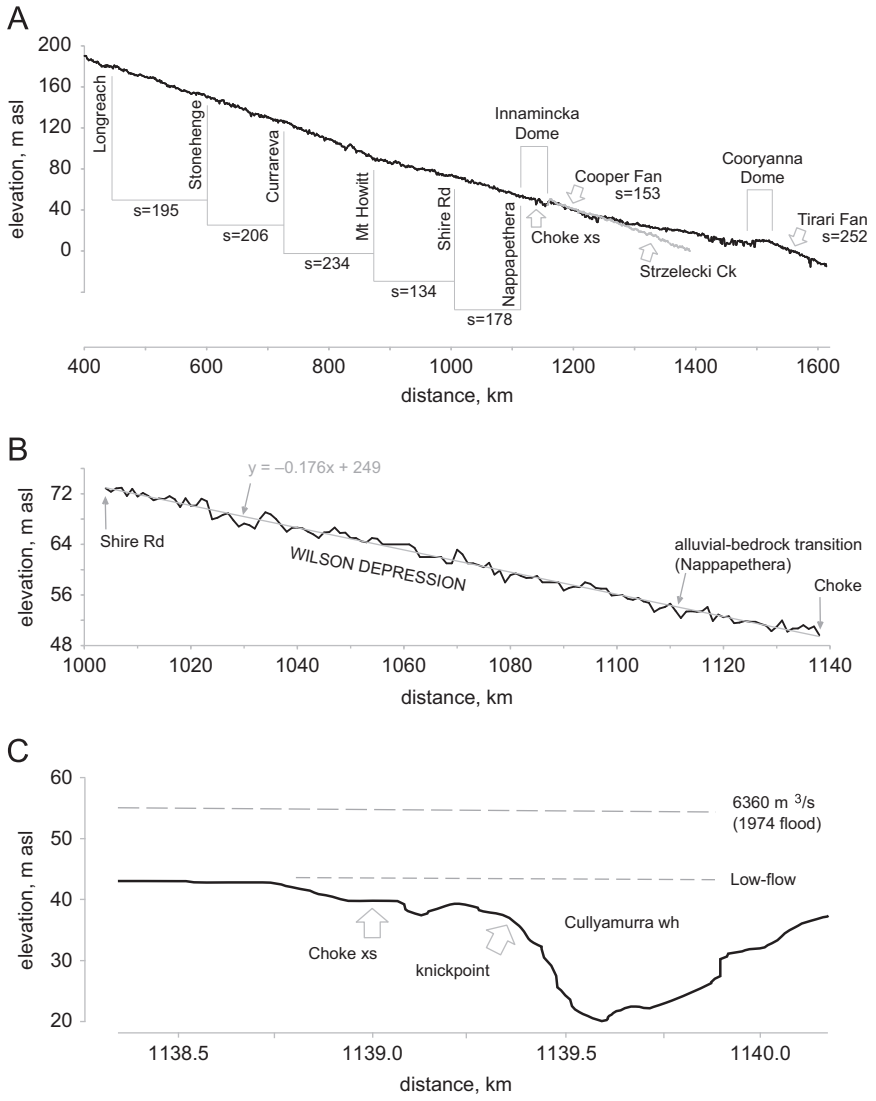

Fig. 3. (A) Cooper Ck long profile derived from SRTM 1 arc-s data, showing mainstem (Longreach to Lake Eyre) and Strzelecki Ck distributary (grey line) at distance from headwater divide. Reach-slopes (s in mm/km) based on linear regression of elevations at 1 km intervals. (B) Detail of stream profile upstream of Innamincka Dome (Shire Rd to Choke, 135 km): constant rectilinear reach slope of 176 ± 3 mm/km (mean $\pm$ 95% confidence interval) via linear regression fitted to elevations at 1 km intervals. (C) Detail of channel bed profile through Cullyamurra waterhole, including pronounced ~18 m-high subaqueous knickpoint revealed via bathymetric survey. The water-surface profile at 6360 m^3/s (1974 flood) was determined with the HEC-RAS hydraulic model.

Nanson, 1986; Nanson et al., 1988; Fagan, 2001; Coleman, 2002; Bowman, 2003; Maroulis et al., 2007; Nanson et al., 2008; Cohen et al., 2010) over an 820 km reach of Cooper Ck from Longreach to Merty Merty (Fig. 1A; note that Longreach is 200 km upstream of the extent shown). The inventory of ages (see Supplementary Data, S3) was subdivided according to facies type: bedload ($n=94$) or overbank floodplain deposits ($n=38$), and long-term deposition rates (with a reduced dataset, see Results) were calculated by dividing depth by basal age assuming a 'zero age' at the surface. The presence of residual TL has been examined, but when converted to an age this rarely equates to more than a few millennia (Nanson et al., 2008, Table 2), which is too small to have a significant effect on deposition rates for the timescales addressed here. The close correlation between 20 duplicate OSL–TL pairs (Supplementary Data, S5) demonstrates that even single-grain aliquot OSL analyses do not produce systematically younger ages than TL.

With the aim of calculating vertical accretion rates of the modern floodplain for comparison to the luminescence-derived rates, concentrations of suspended-load sediment from flow gauges at Currareva and Nappa Merrie (Nappapethera) were converted to a sediment volume delivered overbank to the floodplain each year (Supplementary Data S4).

3.3. Fluvial bedrock incision rates quantified with cosmogenic ^{10}Be

The concentration of in situ-produced cosmogenic nuclides at the Earth's surface is a function of exposure ages and erosion rates (Lal, 1991; Gosse and Phillips, 2001). Surface exposure dating is widely employed to infer the exposure history of landscapes and to quantify the rate of fluvial incision into bedrock (e.g., Burbank et al., 1996; Jansen et al., 2011), though no studies specifically account for episodic plucking at the channel boundary. Four bedrock samples (CH1, -2, -3, -4) were collected for measurement of ^{10}Be in a cross-section spanning fluvially eroded bedrock surfaces at Cullyamurra waterhole—the Choke transect (Figs. 3 and 4) (see Supplementary Data, S5 for full analytical information). The sampled surfaces preserve evidence of fluvial abrasion along with some local spalling and granular disintegration, but we interpret the stepped morphology of the cross-section to be

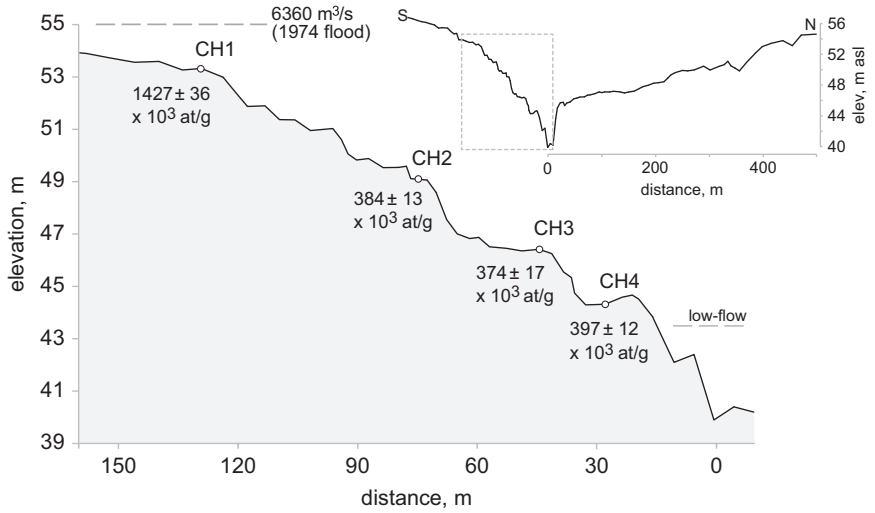

Fig. 4. Cosmogenic nuclide sample transect at the Choke left (south) valley-margin formed in well-jointed silcrete bedrock. Samples span 9 vertical metres from edge of high terrace surface (CH1) down to just above low-flow channel (CH4). The measured ^{10}Be concentrations ($\times 10^3$ atoms/g) are given with 1σ analytical errors (Supplementary Data, S5). The simulated water-surface level for a discharge of 6360 m^3/s (1974 flood) is shown topping CH1. Full valley cross-section is inset.

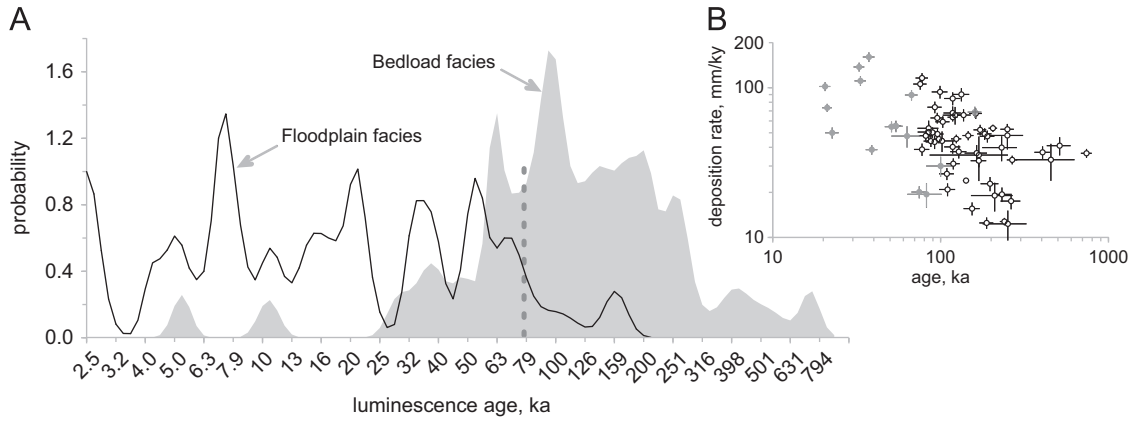

Fig. 5. (A) Luminescence-ages of bedload ($n=49$) and floodplain ($n=37$) sedimentary units (Supplementary Data, S3) on Cooper Ck upstream of Innamincka Dome plotted as kernel density estimates (composite of Gaussian probability curves for each age normalized to unit area). The present-day anabranching channel network is entrenched within a floodplain mud sheet of ~2–6 m thickness, underlain by predominantly sandy bedload facies (Rust and Nanson, 1986)—all dates derive from this relatively uniform stratigraphy. During laterally-active channel phases the mud sheet was reworked across the full valley floor; however, from ~75 ka (denoted by dashed line) lateral migration began to decline, expanding the area of mud sheet preservation and leading eventually to the vertical-accretion floodplain and anabranching river pattern of today. (B) Deposition rate versus age for bedload (black) and floodplain (grey) units, with 1σ errors. As shown here, imposing age-limiting thresholds (>75 ka for bedload, and >20 ka for floodplain units) considerably enhances data reliability by suppressing the scaling that normally exists between deposition rate and measurement interval (Supplementary Data, S3).

chiefly the result of plucking of large silcrete joint-blocks (Fig. 2). The thickness of detached blocks is a function of the spacing of primary horizontal joints in the bedrock, which was estimated by measuring 50 joints in the sample transect.

4. Results

4.1. River profile and modern flood dynamics

Upstream of the Dome the anabranching channel network maintains a remarkably constant reach-slope of 176 ± 3 mm/km (mean $\pm$ 95% confidence interval) over 135 km from Shire Rd to the Choke transect (Fig. 3B). From here the channel steepens along a bedrock-confined reach culminating in an ~18 m-high knickpoint concealed beneath the water-level of Cullyamurra waterhole (Fig. 3C). The knickpoint tip lies 340 m downstream of the Choke, and corresponds to a bedrock-constriction 60 m in width (Figs. 3C and 4). About 17 km further downstream the channel resumes a fully alluvial condition at the Cooper Fan apex and the mainstem flows west with a reach-slope of 153 ± 36 mm/km (mean $\pm$ 95% confidence interval) similar to that above the Dome.

The HEC-RAS model simulations of the 6360 m^3/s discharge ($>$ 100-year flood in 1974) show that the flow hydraulics are strongly influenced by the degree of lateral constriction at the knickpoint. Floodwaters were estimated to be ~15 m deep at the Choke (Figs. 3C and 4), and the zone of water-surface steepening corresponds to the deposits of coarse boulders on flanking bedrock surfaces (Fig. 2). The average intermediate axis of the four largest detached joint-blocks is 900 mm, which according to Komar's (1996) function, Eq. (1), yields a critical shear stress of 461 N/m^2. In comparison, the mean shear stress (cross-section average) predicted by the HEC-RAS model for the 6360 m^3/s discharge at the boulder site was 52 N/m^2, or ~11% of the critical threshold (Supplementary Data, S2). This is probably a crude estimate, given that turbulence around irregular bedrock boundaries can produce widely variable localised flow conditions

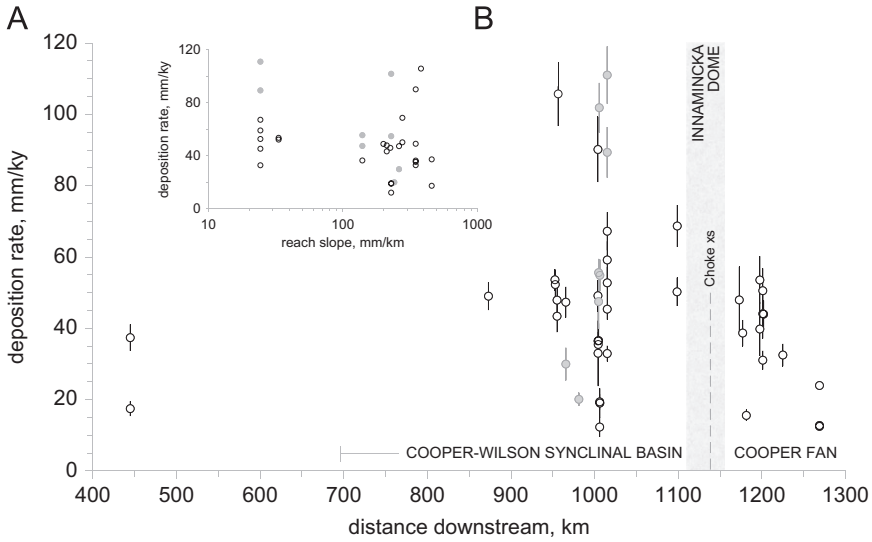

Fig. 6. (A) Downstream distribution of Cooper Ck deposition rates from Longreach (445 km) across Innamincka Dome to Merty Merty (1269 km on the Strzelecki Ck distributary). Open circles are deposition rates (mm/ky $\pm 1\sigma$, $n=38$) derived from bedload sedimentary units >75 ka. Grey circles are overbank deposition rates (mm/ky $\pm 1\sigma$, $n=8$) derived from floodplain sedimentary units >20 ka. Note that one floodplain outlier is not shown: 160 ± 12 mm/ky (at $\sim$962 km). The modern floodplain deposition rate is 48 ± 18 mm/ky, as derived from sediment load data (Supplementary Data, S4). (B) Deposition rate versus channel slope (derived from a 5-km moving window) for bedload units (open circles, $n=23$) and floodplain units (grey circles, $n=8$) upstream of the Innamincka Dome.

(Komar, 1996), but the results strongly imply that the largest joint-blocks at the Choke are mobilised by floods with annual exceedance probability of much less than 1%.

4.2. Deposition rates quantified via OSL–TL dating and sediment load data

The 132 OSL–TL dated sedimentary units are mostly <270 ka and from depths of <12 m, although the oldest age, 740 ± 55 ka, was obtained from a depth of 27 m (Supplementary Data, S3). A frequency analysis based on kernel density estimates of those ages distributed upstream of Innamincka Dome indicates a transition beginning $\sim$75 ka from sandy bedload facies to muddy top-stratum (Fig. 5A); hence, this threshold was chosen as the minimum bounding-age for calculating long-term deposition rates from basal bedload units. Ages <75 ka are excluded because they are considered to be influenced by the transition in river pattern from meandering to anabranching $\sim$75–55 ka. Overbank deposition rates were calculated likewise from dated floodplain units using a minimum bounding age of 20 ka; units <20 ka are excluded because they likely reflect the influence of preservation bias, rather than indicating long-term deposition rates (Lewin and Macklin, 2003). The scaling between deposition rate and its measurement interval is a well known aspect of sedimentary environments (Sadler, 1981; Schumer and Jerolmack, 2009). The age-limiting thresholds (>75 ka for bedload, and >20 ka for floodplain) considerably enhance data reliability by helping to suppress the deposition rate–age scaling (Figs. 5B and 6).

From relatively low, long-term values at Longreach (445 km), deposition rates become more variable downstream along the Cooper–Wilson synclinal basin (Fig. 6A). There is no steady downstream gradation in slope associated with the river profile: both vary widely, as shown by the lack of scaling between deposition rate and channel slope in this reach (Fig. 6B). Downstream of $\sim$870 km (Fig. 6A) and especially in the Wilson depression, deposition rates derived from basal bedload units vary widely from $\sim$12 to 106 mm/ky; floodplain deposition rates reveal similar variation from $\sim$20 to 111 mm/ky, although one outlier is 160 ± 12 mm/ky (at $\sim$962 km, not shown in Fig. 6A). Accepting the broad spread of rates as being representative of the natural variation yields an average long-term deposition rate upstream of the Innamincka Dome of 48 ± 21 mm/ky (mean $\pm 1\sigma$, $n=23$). Likewise, the average overbank deposition rate of 64 ± 33 mm/ky (mean $\pm 1\sigma$, $n=8$, excluding outlier) overlaps with the bedload deposition rate above within one standard error. The modern rate of floodplain deposition derived from sediment load data is estimated at 48 ± 18 mm/ky, which is very close to the long-term rates above (Fig. 6A). Downstream of the Dome deposition rates appear to fall off rapidly to <20 mm/ky, as the sediment load is dispersed into three main distributaries: Cooper Ck main stem, Northwest branch, and Strzelecki Ck.

4.3. Fluvial bedrock incision rates quantified with cosmogenic ^{10}Be

The measured ^{10}Be concentrations on the lower three bedrock surfaces (CH2, -3, -4) are statistically equivalent within 1σ analytical errors, while that at CH1 is several-fold greater (Fig. 4, Table S5-1). Uniform nuclide concentrations measured at CH2, -3, -4 (spanning $\sim$5 m of vertical section) suggest that these surfaces were probably eroded in the same event (or several floods closely-spaced in time) that caused widespread bedrock erosion along the valley margin, rather than being incrementally incised from high to low elevation. The stepped morphology of the sampled transect strongly suggests that large joint-blocks have been episodically plucked, with the minimum depth of plucking probably set by the spacing of primary horizontal joints measured in this study at 67 ± 24 cm (mean $\pm 1\sigma$).

A simple episodic plucking model was developed to explore scenarios consistent with the measured ^{10}Be concentrations by varying the number of joint-blocks detached, and the time interval since detachment (Fig. 7A,B; see Supplementary Data, S5). In brief, the model assumes: (i) the nuclide concentration at CH1 reflects a steady-state bedrock erosion rate of 1.5 mm/ky, and CH2, -3, and -4 are subject to this background erosion rate for their entire exposure history; a rate that is representative of the local silcrete lithology and regional denudation; (ii) nuclide concentrations at CH2, -3, and -4 are the result of episodic plucking of one, two or three joint-blocks (one block is 67 cm

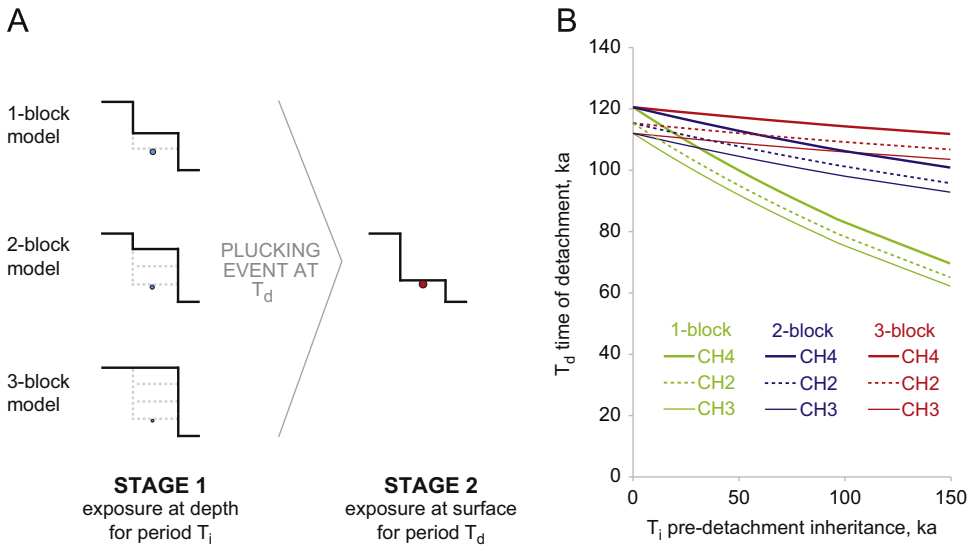

Fig. 7. (A) Schematic outline of the joint-block detachment model showing cosmogenic nuclides accumulating in two stages. For Stage 1, ^{10}Be accumulates relative to shielding depth, as determined by the number of overlying joint-blocks for period T_i—until high-intensity floods detach joint-blocks at time T_d. Nuclide accumulation beneath one, two, or three joint-blocks is denoted by blue dots, whose size indicates the degree of nuclide inheritance. For Stage 2, ^{10}Be accumulates at the exposed surface for period T_d indicated by red dot. The total concentration of ^{10}Be, at the time of sampling, is the sum of inheritance (blue dot) and post-detachment (red dot) components (see Supplementary Data, S5). (B) Results of the joint-block detachment model: time of detachment (T_d) versus pre-detachment interval (T_i) based on ^{10}Be concentrations at CH2, -2, and -3. (For interpretation of the references to colour in this figure legend, the reader is referred to the web version of this article.)

thick); (iii) the timing of block detachment (T_d) was preceded by a period (T_i) in which cosmogenic nuclides accumulated in the sampled surfaces at a depth defined by the thickness of overlying blocks (either 67, 134, or 201 cm); and (iv) cosmogenic nuclides accumulated in the sampled surfaces prior to T_i+T_d are negligible compared to those accumulated during T_i and T_d.

The model computes the timing of block detachment (T_d) for a given pre-detachment plucking interval (T_i) up to 150 ka (Fig. 7B). Maximum T_d indicates the earliest possible plucking episode, 112–121 ka, when T_i is zero (hence inheritance is zero), and the entire nuclide inventory is accumulated during the post-detachment period, T_d. As T_i increases, the proportion of the nuclide concentration attributable to the pre-detachment period grows, and the timing of the last plucking episode becomes younger. This effect on T_d is most pronounced when assuming detachment of a single block; a 67 cm joint-block shields only 68% of the cosmic-ray flux from underlying surfaces, whereas two or three blocks impart greater shielding (90% and 97%, respectively), so the fraction of inherited nuclides in the newly exposed surface is minimal in the latter cases (Fig. 7A, B). The resultant bedrock incision rate is dependent upon the number of joint-blocks detached: modelling one, two, or three blocks yields minimum incision rates of 5.8, 11.6 and 17.4 mm/ky, respectively (Supplementary Data, S5). Given that the cumulative thickness of three joint-blocks (~2 m) approximates the height of bedrock steps between the CH2, -3 and -4 surfaces (Fig. 4), the removal of three blocks together (or in closely-spaced events) poses the most plausible scenario to explain the ^{10}Be concentrations measured on those surfaces. Hence the best estimate of the timing of detachment is close to the mean *maximum* T_d of ~117 ka, implying a *minimum* long-term bedrock incision rate of 17.4 ± 6.5 mm/ky (Supplementary Data, S5).

5. Discussion

5.1. Estimated rates of anticlinal uplift and basin subsidence

Cooper Ck shows no evidence of channel steepening where it first meets bedrock at Nappapethera waterhole and forms a bedrock trench 10 m deep and 250 m wide (Figs. 1 and 3B): a constant rectilinear slope is maintained for 135 km from Shire Rd to the Cullyamurra knickpoint (Fig. 3B). The Cooper has maintained its course across the anticlinal uplift at Innamincka Dome by incising bedrock at a minimum estimated rate of 17.4 ± 6.5 mm/ky, which greatly exceeds the background bedrock denudation rates of ~0.2–5 mm/ky typical of intraplate central Australia (e.g., Bierman and Caffee, 2002; Belton et al., 2004; Heimsath et al., 2010; Fujioka and Chappell, 2011), and our own measurement of 1.5 mm/ky at CH1, which is essentially the rate of bedrock hillslope lowering. Such rates are significantly slower than ^{10}Be-derived fluvial incision rates (~60–120 mm/ky) from the tectonically-active Flinders Ranges to the south (Quigley et al., 2007).

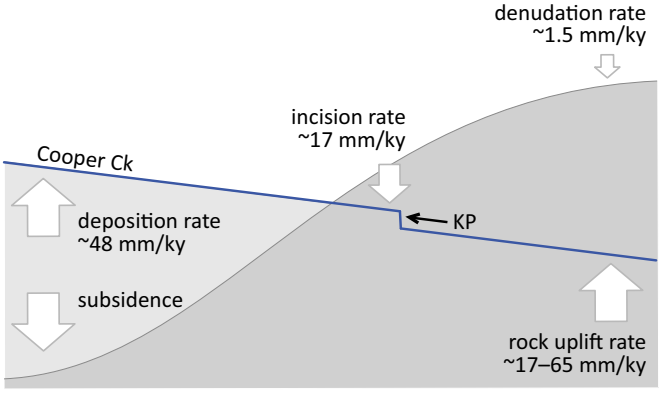

Fig. 8. Diagrammatic sketch of Cooper Ck across the Cooper–Wilson synclinal depression to Innamincka Dome (flow from left to right). Cooper Ck maintains a rectilinear channel slope across the subsiding basin by vertically aggrading. The knickpoint (KP) is in the process of retreating upstream towards the alluvial-bedrock transition at Nappapethera (Fig. 1B).

It is generally the case that steepening and narrowing occurs where an alluvial river meets bedrock due to the increased erosional capacity necessary to erode bedrock (Schumm et al., 2000). Any relative uplift of the Dome should theoretically cause deposition rates to increase as channel slopes decline towards

the rising anticline. The lack of sensitivity of deposition rate to channel slope is unexpected (Fig. 6B), and suggests that something other than slope must be governing sedimentation. One explanation for the decoupling of slope and deposition rate is that surface subsidence is accommodating the thickening valley fill and allowing Cooper Ck to maintain a constant channel slope (cf. Ouchi, 1985). Large seasonal swamps upstream of Nappapethera correspond to the area of widely varying deposition rates (Figs. 1B and 6A), suggesting that spatially non-uniform surface subsidence might be reflecting intra-basinal differences in compaction of the >100 m deep sediment pile.

Surface subsidence coupled with anticlinal uplift separates the aggrading basin upstream from the erosion occurring at the knickpoint and bedrock constrictions, and the magnitude of uplift relative to erosion can be estimated via simple geometric arguments; a schematic overview is presented in Fig. 8. Given that the bedrock channel bed at the Choke lies at 39.9 m asl (Fig. 3C), substantial relative vertical displacement can be deduced from the elevation of the base of the >100 m thick basin-fill (Senior et al., 1978), which lies well below sea level. The absence of channel steepening across the alluvial-bedrock transition suggests firstly that flow constriction provides sufficient boost in erosional capacity to incise bedrock without steepening, and secondly that long-term rates of fluvial incision and uplift must be approximately balanced. The relative contribution of subsidence versus uplift is difficult to constrain with precision, but may be estimated using end-member assumptions as follows. The subsidence-dominant case builds on the condition that the average deposition rate upstream of the Dome (48 ± 21 mm/ky) wholly reflects the accommodation space provided by basin subsidence, hence the fluvial incision rate (17.4 ± 6.5 mm/ky) need only match the equivalent minimum rate of anticlinal uplift: ~ 17 mm/ky. In the case of maximal anticlinal uplift and zero subsidence (with constant valley slope through time), the average basin deposition rate (48 ± 21 mm/ky) plus the rate of fluvial incision (17.4 ± 6.5 mm/ky) gives an uplift rate of $\sim 65 \pm 22$ mm/ky. In other words, back-tilting and the growth of accommodation space associated with anticlinal uplift is the governing control on basin deposition and bedrock erosion.

The Cooper Ck example of anticlinal uplift accompanied by synclinal subsidence poses significant additional complexity to the fault-bound block-uplift model proposed by Humphrey and Konrad (2000). Moreover, our results challenge Humphrey and Konrad's emphasis on the importance of sediment load over stream power concerning the erosional and depositional responses to transverse uplift. Firstly, sediment-driven abrasion is not significant for incision at the Dome; bedrock incision occurs via plucking, as dictated by thresholds of joint-block detachment that are well described by stream power or shear stress (Supplementary Data, S2). Second, extremely slow regional denudation (~ 0.2–5 mm/ky) coupled with aridity produces very low sediment loads, yet the Cooper is still able to fill the accommodation space—maintain a linear stream profile—upstream of the Dome. This suggests that, contrary to Humphrey and Konrad (2000), sediment load is not a rate-limiting control on bed slope in the 'critical region' upstream of the uplift.

Rivers traversing east-central Australia are susceptible even to low rates of surface deformation due to extremely low channel slopes commonly <200 mm/km. The close accordance between folding and regional drainage points directly to the influence of structural control, and only the largest rivers, such as Cooper Ck and Diamantina River, have antecedent reaches that cut transverse to structure (Fig. 1A). Cullyamurra waterhole occupies a bedrock-confined trench that appears to be the product of the headward-retreating knickpoint that now stands at the waterhole's upstream limit (Fig. 3C). We speculate that the knickpoint was initiated at the faulted western margin of the anticline ~ 30 km to the west (Moussavi-Harami and Alexander, 1998). Notable seismicity has occurred in the vicinity of the Dome: 11 earthquakes of magnitude ≥ 3 and two ≥ 4, since the early-1960s (Fig. 1B). Other inferred evidence of recent deformation is the unchannelised reach of Strzelecki Ck at the fan apex (Fig. 1B). The knickpoint is a very pronounced 18 m-high step that dwarfs all other local convexities in the Cooper profile. Ongoing headward retreat to Nappapethera is predicted to instigate a major phase of erosion as the basin-fill upstream adjusts to lower base-level. Previous episodes of base level lowering may explain the fragments of planated bedrock observed at ~ 10 m above the modern channel observed upstream between Nappapethera and the Choke.

5.2. Tectonic and climatic influences on river pattern and sedimentation

Rising base-level is central to most models concerned with the origin and cause of anabranching, especially some well-studied North American examples (Smith and Smith, 1980; Smith, 1983; Makaske et al., 2002), and this notion is further backed by flume experiments (e.g., Ouchi, 1985). Anabranching is not limited to areas experiencing rising base-level (Nanson and Knighton, 1996), though such areas do host some extensive and well developed examples (Nanson et al., 1986). Recent work on the problem focuses upon sediment transport capacity and flow efficiency, with the proposal that division of flow and sediment into multiple channels may be a mechanism for maximising sediment conveyance in low-gradient settings (Jansen and Nanson, 2004, 2010; Huang and Nanson, 2007), or in the case of nonequilibrium systems, for rapidly distributing sediment storage (Tabata and Hickin, 2003; Jansen and Nanson, 2004). Whereas the modern Cooper is a low-energy and predominantly suspended-load anabranching system, the underlying Pleistocene sandy bedload signals a laterally-active meandering river with a bankfull discharge ~ 5–7 times that of today (Nanson et al., 1986, 1988; Rust and Nanson, 1986). In line with flow efficiency arguments, the transition to anabranching between ~ 75 and 55 ka (Fig. 5A) coincided with two factors that both diminish sediment transport capacity: decreasing discharge due to climate, and declining valley slope due to surface deformation. Previous work has attributed the high-energy meandering system to wetter conditions in Marine Isotope Stage-5 (MIS-5: ~ 74–130 ka) and earlier, followed by gradual drying over the last glacial cycle, with tectonism relegated to a secondary role (Rust, 1981; Rust and Nanson, 1986; Nanson et al., 2008). However, in either case the transition to anabranching can be read as a counteract to the fall in sediment transport capacity of the system (Jansen and Nanson, 2004). The anabranching Cooper Ck maintains sediment conveyance across extremely low slopes of ~ 230–180 mm/km (Fig. 3A), despite $>75\%$ transmission losses between Currareva and Cullyamurra waterhole (Knighton and Nanson, 1994). Given the present-day situation in which even the 100-yr flood magnitude is insufficient to achieve significant boulder transport, we surmise that MIS-5 was a time of enhanced discharge on the Cooper with high erosional capacity at the Dome.

5.3. Climate-driven bedrock incision controls long-term sediment storage

How one of the largest river systems in central Australia has maintained course over active structures reveals much about the long-term inputs of sediment and discharge to Lake Eyre, the intra-continental depocentre. The notable absence of a deep sedimentary record at Lake Eyre is difficult to reconcile with its

positioning at the depocentre since the early Miocene (Wells and Callen, 1986). Previous work has invoked deflation during arid playa phases (Magee et al., 2004), but the volume of material contained within the fringing dune fields falls well short of a Neogene depocentre draining ~1.2 million km^2. We propose an alternative explanation in which sediment is sequestered en route to the depocentre: back-tilting has created accommodation space for sedimentation in synclinal basins, while in turn enhancing the rate of vertical accretion by reducing sediment transport capacity (Ouchi, 1985; Holbrook and Schumm, 1999). With 100–150 m of fluvial sands and muds (Senior et al., 1978), the Cooper–Wilson syncline contains ~660–990 km^3 of sediment storage (assuming a prismatic basin geometry) between Currareva and Nappapethera; a volume that dwarfs the 16–40 km^3 of post-Miocene sediments (assuming 2–5 m thickness over 8000 km^2) stored in Lake Eyre today. The syncline therefore acts as an efficient sediment trap, explaining the low sediment delivery to Lake Eyre itself. The Cooper Ck example demonstrates that even where tectonism is relatively modest, synclinal subsidence in the path of lowland arid-zone rivers can foster multiple depocentres that overshadow sediment volumes stored at topographic base level.

The low stream-power that is typical of large, low gradient rivers means that such rivers can in some cases be dependent upon extreme floods to maintain sediment transport capacity (cf. Molnar et al., 2006). The subsiding Cooper–Wilson syncline provides considerable accommodation space for sediments whose partial reworking is governed by the capacity of large floods to lower base-level by incising bedrock obstructions downstream, and in this context geomorphically-effective floods have an annual exceedance probability of much less than 1%. ^{10}Be exposure dating suggests that major bedrock erosion due to high-magnitude floods most likely occurred during MIS-5; timing that corresponds closely with independent OSL–TL evidence of strong fluvial activity indicated by the frequency of dated bedload units (Fig. 5A). The implied absence of Holocene incision at the Choke suggests that fluvial activity in central Australia does not conform to a simple cycle of dry glacial and wet interglacial; rather, continental aridity may be strengthening in the long-term (Nanson et al., 2008). It may be that aridity is underpinning a decrease in the incision rate by suppressing the frequency of large floods (Molnar et al., 2006).

6. Conclusions

Large-scale folding associated with intraplate tectonism is responsible for deformation patterns that steer the regional drainage as well as providing accommodation space for sequestering large volumes of sediment en route to the intra-continental depocentre, Lake Eyre. One such storage, the Cooper–Wilson syncline, contains ~660–990 km^3 of Quaternary sediment accumulated at a rate of 48 ± 21 mm/ky since ~270 ka, while at the same time Cooper Ck has maintained its course across the rising anticlinal limb of Innamincka Dome by incising bedrock at a minimum rate of 17.4 ± 6.5 mm/ky. The rate of Dome surface uplift is bracketed between 17 and 65 mm/ky, but very likely falls closer to the lower end of this range (accounting for a greater proportion of subsidence relative to uplift). The rising bedrock Dome constitutes the local base-level, and thereby governs the valley slope across the subsiding basin; yet, this base-level is ultimately controlled by the rate of bedrock lowering via detachment of joint-blocks during rare, extreme floods. The last big-flood phase occurred no earlier than ~112–121 ka, corresponding to a period of enhanced fluvial activity in central Australia (Nanson et al., 2008). Relative base-level rise coupled with climate-forced reduction in discharge over the last glacial cycle is responsible for the transition in river pattern ~75–55 ka from a bedload-dominant, laterally-active meandering river to the vast, muddy anabranching channel network of today. The entrapment of sediment in such subsiding basins may explain the lack of Quaternary sediment accumulated in the Lake Eyre depocentre, and moreover suggests that notions of a single primary depocentre at base-level may not apply to lowland, arid-zone rivers.

Acknowledgements

This research was funded by a UK Natural Environment and Research Council fellowship (NE/EO14143/1) to Jansen, and Australian Research Council Discovery Grants (DP1096911, DP130104023) to Nanson and colleagues. We thank Sheng Xu for conducting the AMS measurements at the Scottish Universities Environmental Research Centre, R.J. Wasson for comments on an early draft, and E.W. Portenga for an insightful review.

Appendix A. Supplementary materials

Supplementary data associated with this article can be found in the online version at http://dx.doi.org/10.1016/j.epsl.2013.02.007.

References

Adams, J., 1980. Active tilting of the United States midcontinent: geodetic and geomorphic evidence. Geology 8, 442–446.
Alley, N.F., 1998. Cainozoic stratigraphy, palaeoenvironments and geological evolution of the Lake Eyre Basin. Palaeogeogr. Palaeoclimatol. Palaeoecol. 144, 239–263.
Belton, D.X., Brown, R.W., Kohn, B.P., Fink, D., Farley, K.A., 2004. Quantitative resolution of the debate over antiquity of the central Australian landscape: implications for the tectonics and geomorphic stability of cratonic interiors. Earth Planet. Sci. Lett. 219, 21–34.
Bierman, P.R., Caffee, M., 2002. Cosmogenic exposure and erosion history of Australian bedrock landforms. Geol. Soc. Am. Bull. 114, 787–803.
Bowman, H.H., 2003. The flow Hydraulics of Cooper Creek through the Innamincka Dome. Unpublished B.Sc. (Hons) Thesis. School of Geosciences, University of Wollongong.
Burbank, D.W., Leland, J., Fielding, E., Anderson, R.S., Brozovic, N., Reid, M.R., Duncan, C., 1996. Bedrock incision, rock uplift, and threshold hillslopes in the northwestern Himalayas. Nature 379, 505–510.
Cohen, T.J., Nanson, G.C., Larsen, J.R., Jones, B.G., Price, D.M., Coleman, M., Pietsch, T.J., 2010. Late Quternary aeolian and fluvial interactions on the Cooper Creek fan and the association between linear and source-bordering dunes, Strzelecki Desert, Australia. Quat. Sci. Rev. 29, 455–471.
Coleman, M., 2002. Alluvial, Aeolian and Lacustrine Evidence for Climatic and Flow Regime Changes Over the Past 250 ka, Cooper Creek Near Innamincka, South Australia. Unpublished Ph.D. Thesis. School of Geosciences, University of Wollongong.
Fagan, S.D., 2001. Channel and Floodplain Characteristics of Cooper Creek, Central Australia. Unpublished Ph.D. Thesis. School of Geosciences, University of Wollongong.
Fujioka, T., Chappell, J., 2011. Desert landscape processes on a timescale of millions of years, probed by cosmogenic nuclides. Aeolian Res. 3, 157–164.
Galloway, M.C., Senior, D., Cooper, R.D., 1971. Tickalara, Queensland, Sheet SH54-3, 1:250 000 Geological Series. Bureau of Mineral Resources, Geology and Geophysics.
Gosse, J.C., Phillips, F.M., 2001. Terrestrial in situ cosmogenic nuclides: theory and application. Quat. Sci. Rev. 20, 1475–1560.
Gravestock, D.I., Callen R.A., Alexander, E.M., Hill, A.J., 1995. Strzelecki, South Australia, Sheet SH54-2, 1:250 000 Geological Series. Department of Mines and Energy, South Australia, p. 49.
HEC, 1997. HEC-RAS River Analysis System v.2.0. Hydrologic Engineering Centre, United States Army Corps of Engineers, Davis, California.
Heimsath, A.M., Chappell, J., Fifield, K., 2010. Eroding Australia: rates and processes from Bega Valley to Arnhem Land. In: Bishop, P., Pillans, B. (Eds.), Australian Landscapes, 346. Geological Society, London, pp. 225–241 (Special Publications).
Hillis, R.R., Sandiford, M., Reynolds, S.D., Quigley, M.C., 2008. Present-day stresses, seismicity and Neogene-to-Recent tectonics of Australia's 'passive' margins: intraplate deformation controlled by plate boundary forces. In: Johnson, H., Dore, A.G., Gatliff, R.W., Holdsworth, R., Lundin, E.R., Ritchie, J.D. (Eds.), The Nature and Origin of Compression in Passive Margins, 306. Geological Society, London, pp. 71–90 (Special Publications).

Holbrook, J., Schumm, S.A., 1999. Geomorphic and sedimentary response of rivers to tectonic deformation: a brief review and critique of a tool for recognising subtle epeirogenic deformation in modern and ancient settings. Tectonophysics 305, 287–306.
Huang, H.Q., Nanson, G.C., 2007. Why some alluvial rivers develop an anabranching pattern. Water Resour. Res. 43, W07441.
Humphrey, N.F., Konrad, S.K., 2000. River incision or diversion in response to bedrock uplift. Geology 28, 43–46.
Jansen, J.D., Fabel, D., Bishop, P., Xu, S., Schnabel, C., Codilean, A.T., 2011. Does decreasing paraglacial sediment supply slow knickpoint retreat? Geology 39, 543–546.
Jansen, J.D., Nanson, G.C., 2004. Anabranching and maximum flow efficiency in Magela Creek, northern Australia. Water Resour. Res. 40, W04503.
Jansen, J.D., 2006. Flood magnitude-frequency and lithologic controls on bedrock river incision in post-orogenic terrain. Geomorphology 82, 39–57.
Jansen, J.D., Nanson, G.C., 2010. Functional relationships between vegetation, channel morphology, and flow efficiency in an alluvial (anabranching) river. J. Geophys. Res. 115, F04030.
Knighton, A.D., Nanson, G.C., 1994. Flow transmission along an arid zone anastomosing river, Cooper Creek, Australia. Hydrol. Processes 8, 137–154.
Knighton, A.D., Nanson, G.C., 2002. Inbank and overbank velocity conditions in an arid zone anastomosing river. Hydrol. Processes 16, 1771–1791.
Komar, P.D., 1996. Entrainment of sediments from deposits of mixed grain sizes and densities. In: Carling, P.A., Dawson, M.R. (Eds.), Advances in Fluvial Dynamics and Stratigraphy. John Wiley and Sons, Chichester, pp. 127–181.
Kotwicki, V., 1986. Floods of Lake Eyre. Engineering and Water Supply Department, Adelaide. 99 pp.
Lal, D., 1991. Cosmic ray labeling of erosion surfaces: in situ nuclide production rates and erosion models. Earth Planet. Sci. Lett. 104, 424–439.
Lewin, J., Macklin, M.G., 2003. Preservation potential for Late Quaternary river alluvium. J. Quat. Sci. 18, 107–120.
Magee, J.W., Miller, G.H., Spooner, N.A., Questiaux, D., 2004. Continuous 150 k.y. monsoon record from Lake Eyre, Australia: insolation-forcing implications and unexpected Holocene failure. Geology 32, 885–888.
Makaske, B., Smith, D.G., Berendsen, H.J.A., 2002. Avulsions, channel evolution, and floodplain sedimentation rates of the anastomosing upper Columbia River, British Columbia, Canada. Sedimentology 49, 1049–1071.
Maroulis, J.C., Nanson, G.C., Price, D.M., Pietsch, T.J., 2007. Aeolian-fluvial interaction and climate change: source-bordering dune development over the past ~100 ka on Cooper Creek, central Australia. Quat. Sci. Rev. 26, 386–404.
Molnar, P., Anderson, R.S., Kier, G., Rose, J., 2006. Relationships among probability distributions of stream discharges in floods, climate, bed load transport, and river incision. J. Geophys. Res. 111, F02001.
Moussavi-Harami, R., Alexander, E., 1998. Tertiary stratigraphy and tectonics, Eromanga Basin region. MESA J. 8, 32–36.
Nanson, G.C., 1980. A regional trend to meander migration. J. Geol. 88, 107–117.
Nanson, G.C., Knighton, A.D., 1996. Anabranching rivers; their cause, character and classification. Earth Surf. Processes Landforms 21, 217–239.
Nanson, G.C., Rust, B.R., Taylor, G., 1986. Coexistent mud braids and anastomosing channels in an arid-zone river: Cooper Creek, central Australia. Geology 14, 175–178.
Nanson, G.C., Young, R.W., Price, D.M., Rust, B.R., 1988. Stratigraphy, sedimentology and late-Quaternary chronology of the Channel Country of western Queensland. In: Warner, R.F. (Ed.), Fluvial Geomorphology of Australia. Academic Press, Sydney, pp. 151–175.
Nanson, G.C., Price, D.M., Jones, B.G., Maroulis, J.C., Coleman, M., Bowman, H., Cohen, T.J., Pietsch, T.J., Larsen, J.R., 2008. Alluvial evidence for major climate and flow regime changes during the middle and late Quaternary in eastern central Australia. Geomorphology 101, 109–129.
Ouchi, S., 1985. Response of alluvial rivers to slow tectonic movement. Geol. Soc. Am. Bull. 96, 504–515.
Quigley, M., Sandiford, M., Fifield, L.K., Alimanovic, A., 2007. Landscape response to intraplate tectonism: quantitative constraints from ^{10}Be nuclide abundances. Earth Planet. Sci. Lett. 261, 120–133.
Rust, B.R., 1981. Sedimentation in an arid-zone anastomosing fluvial system: Cooper's Creek central Australia. J. Sediment. Petrol. 51, 745–755.
Rust, B.R., Nanson, G.C., 1986. Contemporary and palaeochannel patterns and the late Quaternary stratigraphy of Cooper Creek southwest Queensland, Australia. Earth Surf. Processes Landforms 11, 581–590.
Sadler, P.M., 1981. Sediment accumulation rates and the completeness of stratigraphic sections. J. Geol. 89, 569–584.
Sandiford, M., 2003. Neotectonics of southeastern Australia: linking the Quaternary faulting record with seismicity and in situ stress. In: Hillis, R.R., Muller, D. (Eds.), Evolution and Dynamics of the Australian Plate, 22. Geological Society of Australia Special Publication, pp. 101–113.
Sandiford, M., Wallace, M., Coblentz, D., 2004. Origin of the in situ stress field in southeastern Australia. Basin Res. 16, 325–338.
Sandiford, M., Quigley, M., de Broekert, P., Jakica, S., 2009. Tectonic framework for the Cainozoic cratonic basins of Australia. Aust. J. Earth Sci. 56, 5–18.
Schumer, R., Jerolmack, D.J., 2009. Real and apparent changes in sediment deposition rates through time. J. Geophys. Res. 114, F00A06.
Schumm, S.A., Mosley, M.P., Weaver, W.E., 1987. Experimental Fluvial Geomorphology. John Wiley, New York, 413 pp.
Schumm, S.A., Dumont, J.F., Holbrook, J.M., 2000. Active Tectonics and Alluvial Rivers. Cambridge University Press, Cambridge, 276 pp.
Senior, D., 1969. Durham Downs, Queensland, Sheet SG54-15, 1:250 000 Geological Series. Bureau of Mineral Resources, Geology and Geophysics.
Senior, D., 1970. Barrolka, Queensland, Sheet SG54-11, 1:250 000 Geological Series. Bureau of Mineral Resources, Geology and Geophysics.
Senior, B.R., Mond, A., Harrison, P.L., 1978. The geology of the Eromanga Basin. Bur. Miner. Resour. Bull. 1967, 102.
Smith, D.G., Smith, N.D., 1980. Sedimentation in anastomosed river systems: examples from alluvial valleys near Banff, Alberta. J. Sediment. Petrol. 50, 157–164.
Smith, D.G., 1983. Anastomosed fluvial deposits: modern examples from western Canada. In: Collinson, J.D., Lewin, J. (Eds.), Modern and Ancient Fluvial Systems, Special Publication No. 6 International Association of Sedimentologists. Blackwell Scientific Publications, Oxford, pp. 155–168.
Tabata, K.K., Hickin, E.J., 2003. Interchannel hydraulic geometry and hydraulic efficiency of the anastomosing Columbia River, southeastern British Columbia, Canada. Earth Surf. Processes Landforms 28, 837–852.
Townsend, I.J., Thornton, R.C.N., 1975. Innamincka, South Australia, Sheet SG54-14, 1:250 000 Geological Series. Geological Survey of South Australia.
Waclawik, V.G., Lang, S.C., Krapf, C.B.E., 2008. Fluvial response to tectonic activity in an intra-continental dryland setting: the Neales River, Lake Eyre, central Australia. Geomorphology 102, 179–188.
Wasson, R.J., 1983. The Cainozoic history of the Strzelecki and Simpson dunefields (Australia), and the origin of the desert dunes. Z. Geomorphol. Suppl. 45, 85–115.
Wells, R.T., Callen, R.A. (Eds.), 1986. Australasian Sedimentologists Group Field Guide Series No. 4. Geological Society of Australia, Sydney.
Wopfner, H., Callen, R., Wayne, K.H., 1974. The Lower Tertiary Eyre Formation of the southwestern Great Artesian Basin. J. Geol. Soc. Aust. 21, 17–51.